Morphological analysis of 3D skull models for ancestry estimation

Bruno Andrade, Paulo Dias, Beatriz Sousa Santos
Departamento de Eletrónica, Telecomunicações e Informática
Instituto de Engenharia Electrónica e Informática de Aveiro, IEETA,
Universidade de Aveiro, Portugal

Catarina Coelho*, João Coelho*, David Navega*, Sofia Wasterlain**, Maria Teresa Ferreira*
*Laboratório de Antropologia Forense, Centro de Ecologia Funcional
**Centro de Investigação em Antropologia e Saúde
Departamento de Ciências da Vida,
Universidade de Coimbra, Portugal

***Abstract*— Skull analysis is the main tool used in anthropology to identify several characteristics such as ancestry, gender, and variations between populations. Yet, skull analysis methods used by anthropologists still rely heavily on direct manipulation and measurement of the skulls producing significant inter and intra observer errors. Direct manipulation also involves risks of damaging the specimens while handling. In recent years computer methods for skull analysis that rely on 3D models of skulls acquired with a 3D scanner have been proposed. This approach gives the possibility to perform analysis otherwise not possible, simultaneously easing the overall process of skull analysis and reducing variability. This paper describes the development of automatic and semi-automatic methods for morphological analysis of 3D skull models through the extraction and classification of structures aiming to support the estimation of ancestry. Results with fifty specimens are presented.**

Keywords—3D Models, Feature Detection, Skull Morphology, ancestry estimation

1. INTRODUCTION

Both in forensic anthropology and in the anthropology of past populations, the skull is used to estimate ancestry and sex, using metric and/or morphological approaches [1]. In recent decades there has been a paradigm shift in the field of Anthropology and a trend to standardize the ways in which data is collected has been observed [2]. Computing methods have become more used in Anthropological studies, namely in Virtual Anthropology an approach using data from surface scanning and Computed Tomography [3]. Several recent examples are presented by Rhein and Harvati [4]. However, despite continuing research in this area, some problems still remain, namely: (1) the handling of specimens (a particularly relevant issue in the case of archaeological examples), especially during the metric analysis may cause bone degradation; 2) the low repeatability presented by some methods, particularly morphological approaches; 3) the difficulty of describing complex forms.

A new approach proposed by Dias et al. [5] based on the semi-automatic, interactive analysis of 3D skull models acquired by laser scanning has partially overcome some of the above mentioned issues in the context of craniometric analysis. The work presented in this article is in line with this 3D-model based approach; however, it is focused on a different type of methods relying in morphological analysis. These methods are often criticized for being subjective and strongly influenced by the expert's experience, and would benefit from a more systematic method to perform the analysis, reducing intra- and inter-observer variability, and decreasing the risk of damage.

The work presented in this article was developed by an interdisciplinary team involving anthropologists who contributed to establish priorities concerning the issues to tackle, as well as to design and test the methods. The main contributions are: 1) allowing automated extraction of non-metric characteristics of the skull, potentially reducing variability, 2) allowing the classification of these characteristics according to validated anthropological methods to estimate ancestry while supporting the domain experts along the process of skull analysis avoiding loading them with tedious tasks and reducing the risk of damage.

This paper describes briefly relevant non-metric characteristics and traditional methods to perform skull analysis, as well as a new approach based on 3D digital models of skulls. The methods proposed for the analysis of morphological characteristics are described. The results obtained with a sample of fifty skulls of African and European ancestry are presented and discussed and finally, some conclusions and future work are presented.

2. RELATED WORK

The estimation of the ancestry of an individual based on their skull is typically based on the analysis of craniometric points or the study of morphological characteristics. The skull is the skeletal region where we can find the greatest number of characteristics, allowing the analysis of population affinities [6–9]. Many of the cranial features allow differentiation between two of the major ancestor groups, but they cannot distinguish all of them, which led to the creation of extensive lists of characteristics for more detailed evaluations [10,11]. To address this issue, Hefner [10]

proposed new traits and the development of new combinations of traits in order to allow more detailed morphological analysis. This author identified eleven morphological characteristics that allow the estimation of ancestry in different population groups (African, Native American, Asian and European): the anterior nasal spine (ANS), the inferior nasal opening (INA), the interorbital width (IOB), the malar tuber (TM), the width of the nasal aperture (NAW), the nasal bone contour (NBC), the nasal growth (NO), the post-bregmatic depression (PBD), the supranasal suture transverse palatine (TPS), and the zygomaxillary suture (ZS). The classification of these traits is made by visual comparison with illustrations and, therefore, it is very subjective and difficult to replicate. In order to reduce subjectivity Hefner [10] recommended the observation of images developed by Osteoware (a program developed to aid in the documentation of remains of human skeletons [12]), which allows the evaluation of eleven morphological characteristics that the author found to be the most discriminating in the estimation of ancestry. This is the first program that assists in the classification of morphological characteristics through detailed descriptions, and the presentation of dozens of illustrations. As there is no method or application allowing detection and classification of the characteristics defined by Hefner, one of the objectives of this work is to automate the analysis of some of these characteristics, thus increasing the robustness of the process.

The approach proposed by Dias et al. [5] already provides some automation of the craniometrics analysis of 3D skull models acquired by laser scanning. To implement this approach an application (CraMs) was developed to be an auxiliary for the domain experts to ease, improve and augment their analysis. It makes available measurements defined between characteristic points as in traditional craniometry. Automating parts of the process provides a more systematic method to perform craniometric analysis reducing intra- and inter-observer variability, while alleviating the issue of handling specimens. Moreover, it provides opportunity to devise new measures and types of analysis impossible to perform with traditional methods. CraMs provides measurements defined between craniometric characteristic points. Part of these craniometric points can be detected automatically after a skull alignment procedure; moreover, the application can also help anthropologists identify other points of interest by using their input as an initial estimation. Based on these points, a set of measures is computed, and results obtained by two anthropologists with eight specimens show that the use of CraMs reduced intra- and inter-observer variability [5]. While this work was limited to craniometric measures, the overall approach of analyzing 3D models obtained by laser scanning instead of the specimens may be applied to support anthropologists in other studies with the same benefits of decreasing results variability and avoiding damage. This is an opportunity we decided to pursue in this work

3. Approach and 3D models

Acknowledging the potential of the 3D model-based approach, and the limitation of the previous work for craniometrics analysis, the purpose of this work is to apply the same approach to a different type of skull analysis: the morphological analysis to support ancestry estimation [13].

The 3D models used in this work were acquired using two scanners: a Breuckmann and a NextEngine scanner. The former has a 9μm accuracy, and creates models with around 2 million points; yet it costs approximately sixty times more than the latter, which is relatively low cost, easy to use, has a 125μm accuracy and originates skull models with around 0.4 million points. A lower accuracy in measures could put in jeopardy the usage of the methods by experts that only have access to the NextEngine scanner. Thus, to assess if the results obtained with the models produced by the new scanner were acceptable, measures of the same eight skulls were taken with both scanners. The results show that the error between the craniometrics measurements obtained with the skulls from the two scanners are in line with the typical inter/intra observer obtained from expert measurements [14]. To evaluate the methods 51 specimens from two different archaeological collections including mainly African and European individuals were used.

4. Detecting characteristics for ancestry estimation

The method developed by Hefner to estimate ancestry from skull characteristics is based on human interpretation of drawings and thus suffers from significant subjectivity in the classification of morphological characteristics. Automation would be an important step to remove some subjectivity in the process. This section explains the methods developed to automate the detection of some morphological characteristics defined by Hefner, and how they may be used to classify ancestry of individuals.

After previous discussion with the domain experts, priority was given to the post-bregmatic depression (PBD), and to the anatomical structures of the nasal region, more specifically to the width of the nasal aperture (NAW), and the anterior nasal spine (ANS) that are the most important characteristics. The inferior nasal opening (INA), and the contour of the nasal bone (NBC) were also studied. The lower priority given to the analysis of suture-related characters was due to the fact that many of these sutures are absent due to obliteration (consequence of erosion) [10] or because the 3D models accuracy does not allow their identification [15]. The nasal overgrowth was also not considered as it is composed of very fragile bone pieces and, consequently, is damaged in most cases. The observation of the interorbital width and the malar tubercle depends on the previous location of the sutures reason why these characteristics were neither included in this study. The methods proposed to detect the selected structures take into consideration much *a priori* information concerning the morphology of the skull and their development implied a close collaboration with the domain experts.

4.1. Nasal Aperture Width (NAW)

An important goal of this work was to develop an automatic method to extract the nasal aperture width (NAW) and compare it with the different nasal apertures proposed by Hefner to estimate ancestry [10] (Fig. 1). The solution proposed to detect the nasal structure includes three main

steps: finding useful reference points, detecting other seed points, and finally closing the nasal structure.

Fig. 1. Different types of nasal aperture width (NAW). Adapted from[10].

4.1.1. Find reference points for nasal detection

The first step of the NAW detection process consisted in defining craniometric points that could be used to delimit the nasal opening. After a meeting with the anthropologists, the rhinion (rhi) and the nasospinale (ns) were defined as points of interest to establish the limits of the structure. The rhinion is the lower end of the suture between the nasal bones, and the nasospinale is the lowest point at the inferior edge of the piriform aperture at the base of the nasal spine (Fig. 6). In an aligned skull, they are located on the sagittal plane (an anatomical plane which divides the body into right and left halves, as shown in Fig. 2, left). The detection of these two reference points is performed by analysing the curvature of the cross section of the skull obtained by the sagittal plane (Fig.2, right).

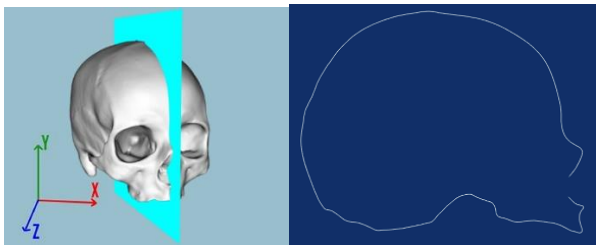

Fig. 2. Sagittal plane containing the Bregma (Left). Cross section resulting from the intersection of the plane with the skull (Right).

In this cross section, rhinion and nasospinale correspond to the points where the curvature changes direction (critical points) (Fig. 3). This condition is combined with a neighbourhood analysis to avoid false detections due to skull degradation. This method provides a list of critical points which include the rhinion and nasospinale; however, due to the degradation state of some skulls, four new conditions based on knowledge about the skull morphology were also considered to select or reject candidates:

- Neighbourhood – analyses the neighbourhood and checks if the critical point results from a progressive change or if it is a local defect. This implies defining the neighbourhood (30 points), which was done empirically based on the 51 specimens used in the study;

- Minimum distance – if any critical points are detected within a given distance, the one with larger slope variation is selected;

- Slope variance – analyses significant changes in slope;

- Discontinuity – situations where the cross section is discontinuous are considered relevant.

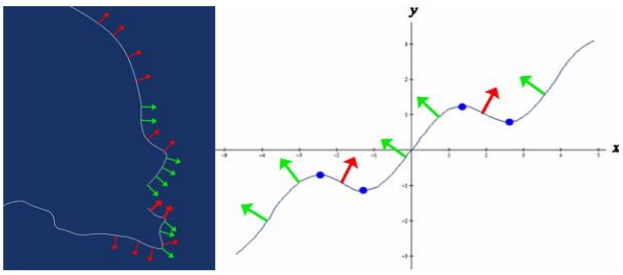

Fig. 3. Normals with positive (red) and negative (green) slope on the cross section (left). Critical points as blue dots (right).

In order to determine the two nasal points (rhi and ns) within the resulting list of relevant points (Fig. 4), the rhinion must be found first as the nasospinale depends on its location. Finding the rhinion is straightforward based on *a priori* craniometric information: it is the point with the highest z-coordinate above a threshold plane. The threshold is defined by the zygion (the most lateral point on the zygomatic arch, which is easily obtained automatically using a method described in [14] (Fig. 5).

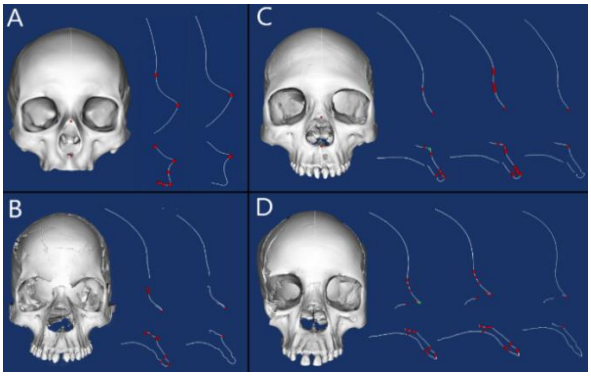

Fig. 4. Skulls with different characteristics and the relevant points.

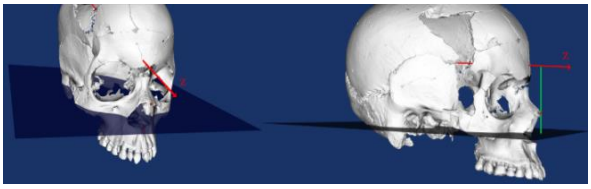

Fig. 5. Plane containing the zygion used to delimit the search areas to find rhinion (located above the plane) and nasospinale (located beneath the plane).

The nasospinale is defined as the point having y-coordinate (ns_y) less than the y-coordinate of the zygion point, simultaneously corresponding to the highest value of the *factor* given by equation (1); this corresponds to minimizing the distance (d) between the rhinion and nasospinale, using the nasospinale ordinate (ns_y) to ensure the point is not detected inside the structure.

$$factor = \frac{ns_y}{d} \quad (1)$$

4.1.2. Detection of other seed points

Considering that the nasal opening (NAW) is the most salient region between the rhinion (rhi) and the nasospinale (ns) it is possible to compute its midpoint (blue dot in Fig. 6, left) and use it as a seed to extract the nasal region. The rhi and ns will be used as boundary references.

A radial search algorithm with spatial partitioning is used to find approximately equidistant seed points defining the nasal structure. The bounds are created by planes perpendicular to the xy-plane, including the midpoint point at their intersection, and making congruent angles between them (Fig. 6, right). The points are detected analysing each point of the surface model with y-coordinate less than the rhinion y-coordinate (rn_y), and looking for the point with the highest z-coordinate in each region (Fig. 7).

Preliminary tests showed that the method failed in skulls with marked prognathism (anterior projection of the jaw, a characteristic very common in individuals of African ancestry), which have a jaw more protruding than the nasal structure (Fig. 8). As this issue affected only the lower points of the nasal opening, a region was defined where the points would only be considered if they intersect a sphere centred at the midpoint of the nasal opening, and passing at the nasospinale (Figure 9). This region is delimited by two planes parallel to the xz-plane (y=0), using a threshold characterized by a distance to nasospinale established empirically. This improvement made the algorithm more robust and effective for skulls with prognathism (Fig. 10).

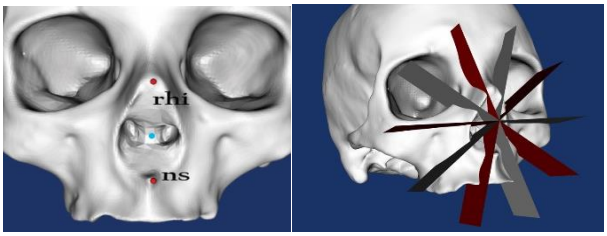

Fig. 6. Nasospinale (ns), rhinion (rhi) and the nasal opening midpoint (left). Section bounds to search for other seed points (right).

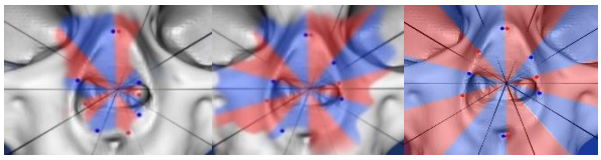

Fig. 7. Searching for the point with the largest z-coordinate in different sections.

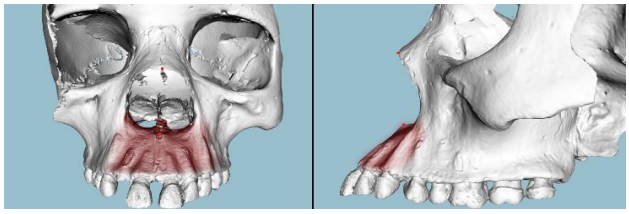

Fig. 8. Skull with prognathism - jaw having a wider projection than the nasal structure (red area).

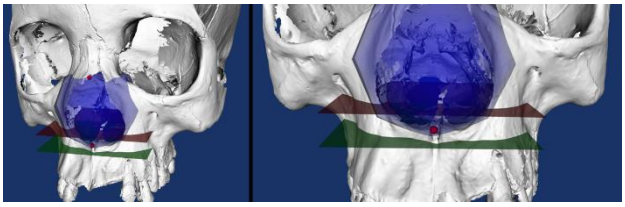

Fig. 9. To solve the prognathism issue only points simultaneously inside the reference sphere (blue) centered at the midpoint of the nasal opening and between the two planes (red and green) at a distance of the nasospinale are considered.

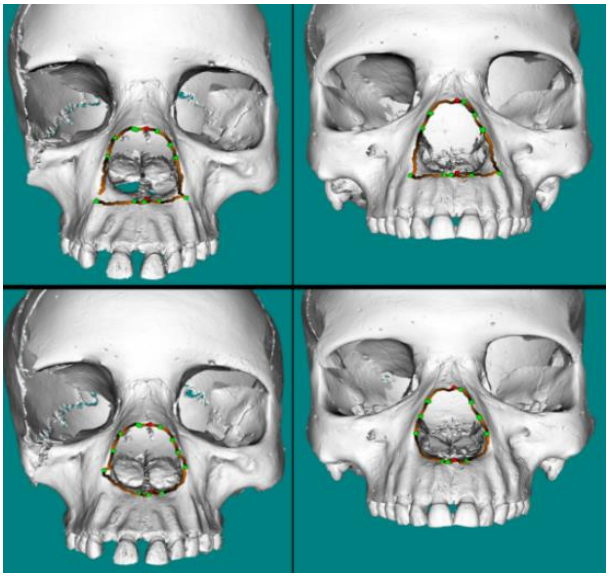

Fig. 10. Seed points detected in skulls with marked prognathism with the first version of the method (top) and with the improved version (bottom). The bottom nasal seeds (green).

4.1.3. Closing the nasal structure

After tests to evaluate the adequate number of seeds (empirically set at 12), it is necessary to detect the nasal boundary. To close the nasal structure a curvature based method previously developed [15] was adapted and used. The method was initially used to detect the orbits, closing a contour using seed points and analysing their neighbourhood. Results for the nasal structure of a case are shown in Fig. 11.

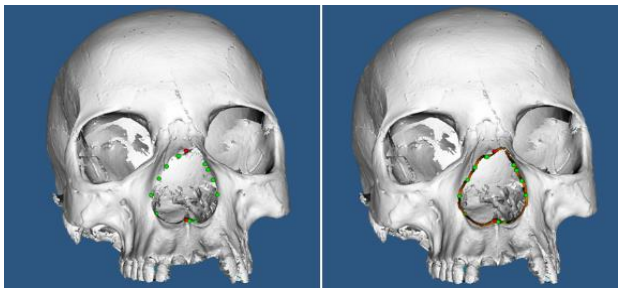

Fig. 11. Seed points (left) and closed nasal structure (right).

4.1.4. Classification of the nasal opening

The extracted nasal contour is a 3D polygon. To allow comparison with the Hefner's 2D profiles [10], the polygon vertices are projected onto the coronal plane (dividing the body into front and back or ventral and dorsal) resulting in a 2D representation of the nasal contour (Fig. 12).

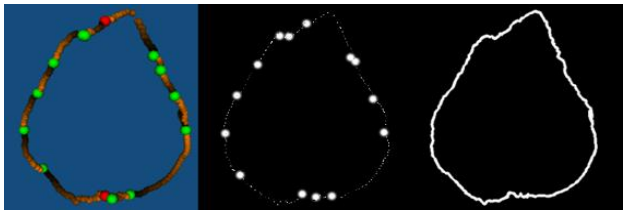

Fig. 12. Obtaining a 2D image from a 3D nasal structure.

The obtained 2D representation of the structure is compared with the original Hefner profiles corresponding to different ancestry types [10]. To allow a direct

comparison, the Hefner profiles are centred and scaled according to the height of the 2D representation of the detected structure (Fig. 13). Finally, the Euclidean distance between each point of the 2D representation of the nasal contour and the closest point on each original profile are calculated.

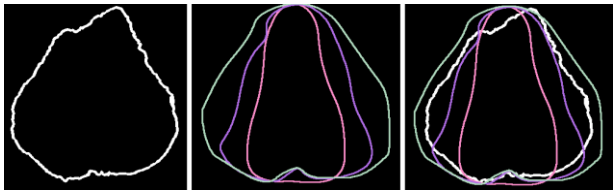

Fig. 13. 2D representation of a specific nasal contour (left), overlapping the nasal profiles of three types of ancestry according to Hefner [7] (middle), all images to identify the closest match (right).

The probability of belonging to each ancestry type is obtained by computing the average distances between each pair of images (obtained 2D representation of the nasal contour and Hefner's profile for each type of ancestry) according to equation (2).

$$p_x = \frac{d_1 + d_2 + d_3}{d_x^3 \times \sum_{i=1}^{3} \frac{d_1 + d_2 + d_3}{d_i^3}} \times 100 \qquad (2)$$

Where p_x is the probability of belonging to type *x*, *dx* is the mean Euclidean distance to the profile corresponding type x and *d1*, *d2*, *d3* are the mean Euclidean distances to the respective Hefner profile.

4.2. Postbregmatic Depression (PD)

The postbregmatic depression is a morphological characteristic observed in the lateral profile of the skull, which can be classified as present or absent [10] (Fig. 14). To assess if this characteristic is present or absent in a skull, a 2D profile is obtained based on a projection of the skull on a sagittal plane (see Fig. 15). The external contour of this profile is obtained and the points between the bregma (A) and the point having the highest y-coordinate posterior to the bregma (B) are analysed to determine their position relatively to the straight line defined by A and B. This allows classifying the PD as present or absent (Fig. 16).

Fig. 14. Postbregmatic depression absent (left) and present (right). Adapted from Hefner [10].

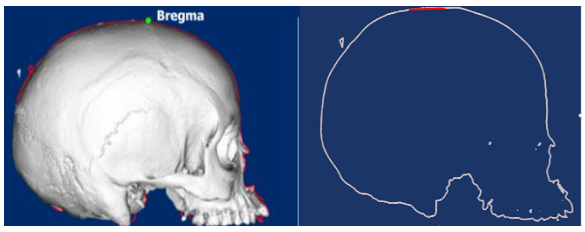

Fig. 15. Skull projection on a sagittal plane, and external contour.

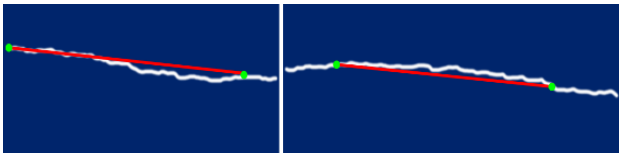

Fig. 16. Assessing if the majority of points are over or under an imaginary line between bregma and highest y-coordinate posterior to the bregma. If the majority of points are under the line, the postbregmatic depression is classified as absent (right), otherwise, it is classified as present (left).

4.3. Anterior Nasal Spine (ANS)

The anterior nasal spine can be classified as absent, medium, or long [10] (Fig. 17). The classification is based on the analysis of the projection of the transition from the nasal floor to the vertical part of the jaw, which occurs in the nasospinale region. As such, the method developed to evaluate this characteristic is based on the position of the nasospinale (obtained as explained in section 4.1.1) and the analysis of the cross section resulting from a cut made by the plane parallel to xz-plane passing through the nasospinale (Fig. 18). If all the points have the z-coordinate superior to the nasospinale, ANS is present; otherwise it is classified as absent (Fig. 19). In order to differentiate medium and long ANS cases, condition (2) is used. If the projection is outside the area defined by (2), ANS is designated as medium, otherwise it is long (Fig. 19). The values that define the area (t*y* and t*z*) were adjusted empirically.

$$P_y > N_y - t_y \quad \cap \quad P_z < N_z - t_z \qquad (1)$$

where: P*z* and P*y* are the coordinates of the point being analysed. N*z* and N*y* are the nasospinale coordinates.

Fig. 17. Different types of nasal spine morphology: 1-absent (left), 2-medium (middle) and 3- long (right). Adapted from Hefner [10].

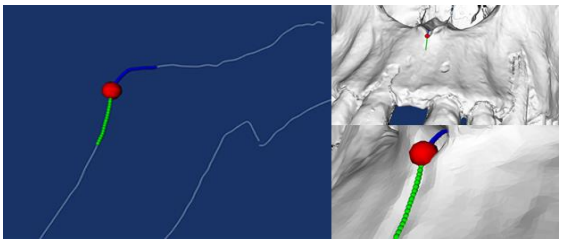

Fig. 18. Skull (right) and the cross-section resulting from the plane parallel to yz-plane containing the nasospinale (left). The red dot marks the nasospinale, and the blue and green dots are the points less than five millimetres away from the nasospinale.

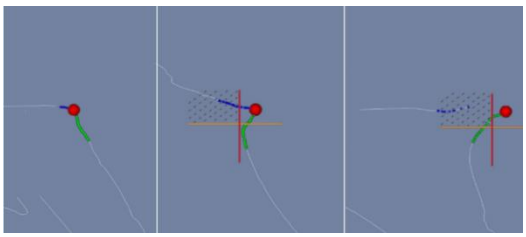

Fig. 19. Classification of the ANS as absent (right), medium (middle) and long (left). The axes and the dashed lines represent the area that allows differentiate the medium from the long cases.

4.4. Ancestry estimation

The study conducted by Hefner [10] relates the frequency distribution of each characteristic with ancestry estimation. Using Hefner's method and based on the detected characteristics, the probability of a skull pertaining to each population group is provided. Using this functionality, domain experts can obtain an estimation of the ancestry classification of an individual automatically or introducing manually some information if necessary (Fig. 20).

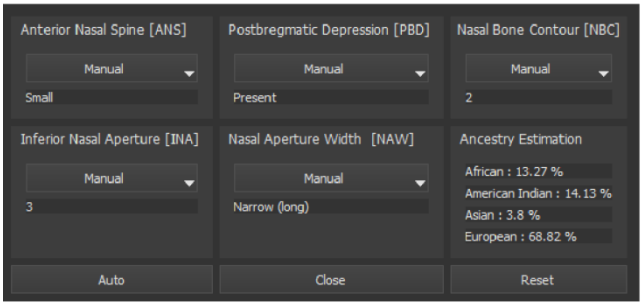

Fig. 20. Supporting ancestry estimation based on the skull non-metric traits studied in this work (using the methods developed or manually).

5. Results and Discussion

This section presents some results obtained with the methods developed for ancestry estimation. The tests were done with 51 specimens from two different collections, the CEI/XXI and the PAVd [16,17]. The validation was performed by comparing the automatic methods results with the evaluation of two domain experts who classified the same specimens using the traditional method (visual comparison with the original Hefner figures [10]).

5.1. Nasal Aperture (NAW)

Three of the 51 skulls were too damaged to be processed and were not used in this study. Concerning the other skulls, an overall success rate of 85% was observed in the identification of nasal aperture width. However, in 9% of the cases the rhinion points and in 4% the nasospinale points could not be detected automatically and were manually marked. A 95% success rate was obtained for the identification of type 3 structures, 100% for type 2, and 71% for type 1 structures (Table 1).

It should be noted that twenty-one models were classified as type 3, nine as type 2 and seventeen as type 1 by the anthropologists. The model CEIXXI_079 was the only one in which there was disagreement between the two anthropologists. The cases in which the rhinion/nasospinale detection fails were mainly due to poor preservation state of some skulls (having fragmented regions) causing an incorrect identification of the two craniometric points and/or in the classification of the structure.

5.2. Postbregmatic Depression (PD)

Forty-five models were used to evaluate the proposed method to identify the postbregmatic depression (PD), as six of the models were too poorly preserved to be classified either manually or using the method described. The classification of post-bregmatic depression presented a 100% agreement with the anthropologists in the cases in which it could be evaluated. Although the method proposed yields promising results, more models with this trait should be studied in order to guarantee the efficacy of the method, since the depression was only present in three specimens.

5.3. Anterior Nasal Spine (ANS)

Forty-one models were used to evaluate the anterior nasal spine classification, as ten specimens could not be classified, neither manually nor using the method due to fragmentation.

Table 1 – Results of the NAW classifications performed according to the traditional method (Manual) and the developed method (Auto). The probabilistic precision of the classification is also given, that is, the percentage for each of the three types, using equation (2).

ID	NAW Manual	NAW Auto	%		
			1	2	3
PAVd'_020	3	3	1	5	94
PAVd'_021	3	3	2	30	68
PAVd'_025	3	3	2	6	92
PAVd'_038	2	2	4	84	12
PAVd'_039	3	3	0	3	97
PAVd'_041	3	3	0	3	97
PAVd'_057	3	3	1	11	88
PAVd'_063	2	2	5	92	3
PAVd'_065	3	3	3	10	87
PAVd'_066	3	3	0	2	98
PAVd'_067	3	3	0	1	99
PAVd'_069	3	3	0	1	99
PAVd'_075	3	3	2	15	83
PAVd'_077	3	3	3	25	72
PAVd'_078	3	3	9	22	69
PAVd'_081	3	3	0	1	99
PAVd'_082	3	3	0	0	100
PAVd'_093	3	3	1	5	94
PAVd'_095	3	3	1	4	95
PAVd'_110	3	3	3	28	69
PAVd'_133	3	3	0	12	88
PAVd'_163	3	2	1	99	0
PAVd'_169	3	3	0	5	95
CEIXXI_002	1	1	11	83	6
CEIXXI_003	1	1	72	26	2
CEIXXI_005	1	1	82	17	1
CEIXXI_006	1	2	30	66	4
CEIXXI_009	1	2	11	88	1
CEIXXI_011					
CEIXXI_013					
CEIXXI_014	2	2	29	60	11
CEIXXI_017	1	2	7	77	16
CEIXXI_018	1	1	96	3	1
CEIXXI_019	1	1	74	24	2
CEIXXI_023	1	1	55	42	3
CEIXXI_024					
CEIXXI_026	1	1	67	31	2
CEIXXI_027	1	1	78	20	2
CEIXXI_028	1	1	69	28	3
CEIXXI_036	2	2	14	77	9
CEIXXI_040					
CEIXXI_050	1	2	22	75	3
CEIXXI_069	1	2	17	80	3
CEIXXI_071	2	2	22	69	9
CEIXXI_072	1	1	73	25	2
CEIXXI_076	1	2	14	83	3
CEIXXI_079	2/1	2	14	80	6
CEIXXI_088	2	2	5	91	4
CEIXXI_092	2	2	6	61	33
CEIXXI_133	1	2	14	84	2
CEIXXI_135	2	2	6	89	5

Ten of the models corresponded to type 1 (ANS absent), nineteen to type 2 (medium) and twelve to type 3 (long). The results of ANS classification using the developed method, compared with the classification made by the anthropologists, showed a success rate of 93% in identifying correctly the structure. The three incorrect classifications resulted from inappropriate differentiation between types 2 and 3, which may be due to fragmentation of the models (Table 2). To ensure the efficacy of the method in the discrimination between types 2 and 3 ANS, more models with these two types should be used. Additionally, the method is very sensitive to the nasospinale position; small errors can result in different classifications and thus the anthropologist should confirm the position of landmark before using the method.

TABLE 2 - ANS classification using manual and automatic methods.

ID	*ANS Manual*	*ANS Auto*
PAVd'_020		
PAVd'_021	1	1
PAVd'_025	1	1
PAVd'_038	2	2
PAVd'_039	1	1
PAVd'_041		
PAVd'_057		
PAVd'_063		
PAVd'_065	1	1
PAVd'_066	2	2
PAVd'_067	1	1
PAVd'_069	1	1
PAVd'_075	1	1
PAVd'_077	2	2
PAVd'_078	1	1
PAVd'_081	2	2
PAVd'_082	2	2
PAVd'_095		
PAVd'_110	3	3
PAVd'_133		
PAVd'_163	1	1
PAVd'_169	1	1
CEIXXI_002	3	3
CEIXXI_003	2	2
CEIXXI_005	3	3
CEIXXI_006	2	2
CEIXXI_009	3	2
CEIXXI_011		
CEIXXI_013	2	2
CEIXXI_014	2	2
CEIXXI_017	2	2
CEIXXI_018	3	3
CEIXXI_019	2	2
CEIXXI_023		
CEIXXI_024		
CEIXXI_026	2	2
CEIXXI_027	3	2
CEIXXI_028	2	2
CEIXXI_036	3	3
CEIXXI_040		
CEIXXI_050	3	3
CEIXXI_069	2	2
CEIXXI_071	2	2
CEIXXI_072	3	3
CEIXXI_076	3	2
CEIXXI_079	3	3
CEIXXI_088	2	2
CEIXXI_092	2	2
CEIXXI_133	2	2
CEIXXI_135	3	3

6. CONCLUSIONS AND FUTURE WORK

This paper presents a set of methods developed to automatically classify morphological characteristics of skulls based on 3D models acquired through laser scanning. The final objective is to help anthropologists to estimate the ancestry of individuals. These methods were tested with 51 3D models of skulls of different ancestry (African and European) with promising results. Although the methods still require validation with more skulls (namely with different ancestry) to ensure their effectiveness, the results suggest that this type of analysis is feasible and obtains results analogous to a traditional analysis, while automating the process, making it easier and possibly more repeatable. It should be noted that these results reinforce the potential of the 3D model based approach in anthropological studies of the skull.

The next step will be to develop methods to classify other morphological structures of the skull. Moreover, since specimens are often fragmented, a method to help align the fragments and reconstruct the mesh in the missing areas would be of great utility. Further improvements of the initial skull alignment method (currently based on a single aligned template and the ICP method) by using a database of template models already aligned would improve the results.

REFERENCES

[1] DiGangi EA, Hefner JT. Ancestry estimation. Res Methods Hum Skelet Biol 2013:117–49.

[2] Davy-Jow SL, Schofield D. Virtual Forensic Anthropology: Applications of Advanced Computer Graphics Technology to the Identification of Human Remains. H. Hao Yang S. Chi-Yin Yuen Handb. Res. Pract. Outcomes Virt. Worlds Env. IGI Glob., 2012.

[3] Weber GW, Schäfer K, Prossinger H, Gunz P, Mitteröcker P, Seidler H. Virtual anthropology: the digital evolution in anthropological sciences. J Physiol Anthropol Appl Human Sci 2001;20:69–80.

[4] Rein TR, Harvati K. Geometric morphometrics and virtual anthropology: advances in human evolutionary studies. Anthropol Anz 2014;71:41–55.

[5] Dias P, Neves L, Santos D, Coelho C, Ferreira MT, Santos H, et al. CraMs: Craniometric Analysis Application Using 3D Skull Models. IEEE Comput Graph Appl 2015;35:11–7.

[6] Brues A. The once and future diagnosis of race. Gill, G. W.; Rhine, S. Skelet. Attrib. race methods forensic Anthr.., Maxwell Museum of Anthropology, Un. of New Mexico; 1990, p. 1–7.

[7] Byers SN. Introduction to Forensic Anthropology. 4th ed. Pearson; 2011.

[8] Gill GW. Craniofacial Criteria in the Skeletal Attribution of Race. Reichs, K.J. Forensic Osteol. Adv. Identif. Hum. Remain. 2nd ed., Illinois: Charles C. Thomas Publisher; 1998, p. 293–315.

[9] Klepinger LL. Fundamentals of Forensic Anthropology. Wiley; 2006.

[10] Hefner JT. Cranial Nonmetric Variation and Estimating Ancestry. J Forensic Sci 2009;54:985–95.

[11] Rhine S. Skeletal Criteria for Racial Attribution. NAPA Bull 2008;13:54–67.

[12] osteoware n.d. https://osteoware.si.edu (assessed May/20/2018).

[13] Andrade B, Dias P, Santos BS, Coelho C, Coelho J, Navega D, et al. Towards automatic non-metric traits analysis on 3D models of skulls. 23° Enc. Port. Comput. Gráfica e Interação, 2016, p. 91–8.

[14] Andrade B. Towards automatic non-metric traits analysis of skulls based on 3D models. MSc Thesis, Un. of Aveiro, 2016.

[15] Neves L. Measures and detection of morphology for craniometry using 3D models. MSc Thesis, Un. of Aveiro, 2014.

[16] Ferreira MT, Vicente R, et al.. A new forensic collection housed at the University of Coimbra, Portugal: The 21st century identified skeletal collection. For Sci Int 2014;245:202.e1-202.e5.

[17] Coelho C. Uma identidade perdida no mar e reencontrada nos ossos : Avaliação das afinidades populacionais de uma amostra de escravos dos séc. XV-XVI. MSc thesis, Univ. of Coimbra, 2012.